Meteorol. Atmos. Phys. 68, 57–77 (1998)

Meteorology and Atmospheric Physics

[1] Centre for Atmospheric Sciences, Indian Institute of Technology, Hauz Khas, New Delhi, India
[2] National Centre for Medium Range Weather Forecasting (NCMRWF), Mausam Bhavan Complex, Lodi Road, New Delhi, India
* Current Affiliation: IBM Solutions Research Centre, Indian Institute of Technology, Hauz Khas, New Delhi, India

Mean Dynamical Characteristics of the Asian Summer Monsoon with a Global Analysis – Forecast System

P. L. S. Rao[1,*], **U. C. Mohanty**[1], and **K. J. Ramesh**[2]

With 16 Figures

Received October 2, 1997
Revised June 26, 1998

Summary

The dynamical characteristics of Asian summer monsoon are examined with a global spectral model. In addition to the seasonal circulation features, the large scale budgets of kinetic energy, vorticity and angular momentum are examined making use of mean analysis and forecast fields (upto day 5) for summer season comprising June, July and August, (JJA) 1994. Apart from elucidating the systematic errors over the monsoon region, the study expounded the influence of these errors on associated dynamics.

The significant errors in the low level flow (850 hPa) evince (i) weakening of south easterly trades and cross equatorial flow into the Northern Hemisphere and (ii) weakening of westerly flow over the North Indian Ocean. Similarly, in the upper level flow (200 hPa) they indicate (i) weakening of Tibetan anti-cyclone and (ii) reduction of return flow into the Southern Hemisphere.

The balance requirements in the mean analysis as well as forecast fields are fairly in agreement with the observed over the summer monsoon. The monsoon domain is discerned as the source region of kinetic energy and vorticity. Both are produced in the monsoon region and transported horizontally across. The model forecasts fail to retain the analyzed atmospheric variability in terms of mean as well as transient circulations which is revealed by kinetic energy budget. This is further corroborated by vorticity and angular momentum budgets. It is noticed that the forecasts in all ranges produce feeble monsoon circulation which weakens considerably with increase in the forecast period.

1. Introduction

The Asian summer monsoon represents conspicuous changes in the general circulation of the atmosphere characterized by periodic reversal of wind regimes, movements of jet streams and semi-permanent high/low pressure areas. The monsoon circulation is triggered by a sequence of events. Succinctly, the formation of heat low precedes moisture convergence, which is followed by heat flux convergence (Mohanty et al., 1983). Both in turn give rise to profound cumulus convection and enhanced diabatic heating. This enables generation of available potential energy (APE). Ultimately the circulation gets established through conversion of APE to kinetic energy (KE) and noticed by sudden rise in kinetic energy (Krishnamurti et al., 1981; Pearce and Mohanty, 1984) over the Arabian Sea. The advent of several field experiments over the monsoon region entails the comprehensive understanding of various complex mechanisms to ameliorate its simulation/prediction. The prominence of the diagnostic studies in elucidating the dynamics of tropics is well recognized as an important GARP problem (Kung and Smith, 1974; Pearce, 1979). The paucity of data made the myriad nuances of the summer monsoon unexplained and recondite unlike the data rich mid-latitude regions. However, the abundant availability of globally analyzed upper air meteorological fields from various operational weather forecasting centres in the recent times has improved the understanding considerably.

It is known that all numerical models drift towards their preferred climatology as the forecast period increases, and such tendency dominates forecast errors. The monsoon region is on exception to these prediction errors. The diagnosis of the source of these errors associated with simulation/prediction of the summer monsoon is an integral part of the refinement of the forecast model. The major part of these systematic errors in the numerical models are attributed to improper representation of sub-grid scale physical processes such as boundary layer, convection, radiation and land surface processes etc. and their complex interactions. These processes are generally represented by the expressions of certain conceptual formulations of unresolved scales of motion in terms of resolvable scales. Therefore, comprehensive knowledge of physical processes which influence and control the maintenance of the summer monsoon and the necessary improvements in various parameterization schemes to represent them suitably in the general circulation models are imperative to improve the forecast skill.

The tropical systematic errors of the European Centre for Medium Range Weather Forecasts (ECMWF) model were analyzed (Heckley, 1985a and b; Kanamitsu, 1985; Rabier et al., 1996) and their dependence on parametrization of physical processes was amply demonstrated (Tiedke et al., 1988; Slingo et al., 1988). A substantial reduction of errors in the prediction of large scale tropical circulation was observed after introducing certain improvements in the physical parametrization schemes at the ECMWF (Mohanty et al., 1995a). Most of these studies revealed the error characteristics over the monsoon domain. Nevertheless, none has dealt with the effect of these errors on the dynamics of the monsoon, in particular, the large scale balances which ought to be satisfied in various time scales. An endeavor is made to diagnose the errors and explain how these errors contaminate seasonal dynamical features.

In this study, the seasonal scale systematic errors of a global spectral model operational at the National Centre for Medium Range Weather Forecasting (NCMRWF), New Delhi, over the Asian summer monsoon region are examined in detail. Further, the influence of these errors on the circulation features and associated dynamics is investigated through the comprehensive analysis of large scale budgets of kinetic energy, vorticity and angular momentum. In this process, the performance of the model is assessed based on the fulfillment of these balances at different forecast ranges.

2. Data and Computational Procedure

A global data assimilation and forecast system to provide medium range forecasts is operational at the NCMRWF, New Delhi since June 1, 1994 (Mohanty et al., 1995b). An intermittent type of assimilation at 6-hourly interval is used for maximizing the data input. In the analysis cycle, however, data received within a 3-hourly period on either side of the analysis hour are included for assimilation. The global data assimilation and forecasting system of the NCMRWF are adapted from the National Centers for Environmental Prediction (NCEP), Washington D.C., USA. The data assimilation system is based on spectral statistical interpolation (SSI) scheme. The forecast model has horizontal resolution of T-80 with 18 layers in the vertical. The details of the assimilation system and forecast model are documented in earlier studies (Parrish and Derber, 1992; Kanamitsu, 1989).

The data base employed in this study consists of 0000 UTC operational analyses and forecasts (day 1 through day 5) of the NCMRWF for the summer monsoon season (June-August) of 1994. The meteorological data considered for the study include wind and geopotential fields over the summer monsoon region extending from 15° S to 45° N latitudes and 30° E to 120° E longitudes at ten pressure levels (1000, 850, 700, 500, 400, 300, 250, 200, 150, 100 hPa) having horizontal resolution of 1.5° latitude/longitude. The mass and velocity fields are analyzed by four dimensional data assimilation scheme in which, the assimilation is carried out in three different steps, viz. complex quality control, spectral statistical interpolation, and six hour forecast, which provides the first guess in order to carry out the subsequent analysis. In this study, the vertical component of the motion is estimated by a kinematic technique with vertical adjustment of divergence over each column as suggested by O'Brien (1970).

The authors have examined the error characteristics through various case studies making use of 1994 as well as 1995 data. The errors are similar in nature. Further, the global data assimilation forecast system (GDAFS) remained invariant since 1 June, 1994, we intend to present detailed discussion pertaining to one of them. The results for the monsoon season of 1994 are presented as the monsoon of 1994 is significant because of the fairly normal distribution of rainfall throughout Indian subcontinent.

The budget equations are obtained from atmospheric model equations with simple mathematical transformations (Haltiner and Williams, 1980; Holton, 1992). The following are the various budget equations used in the present study and all of them are expressed in flux form involving pressure coordinate in the vertical. The over bar in the budget equations denote the mean value of a quantity for the season (JJA) and prime quantities denote their corresponding deviation from the seasonal mean.

2.1 Mean Kinetic Energy Budget Equation

$$\overline{\frac{\partial K_M}{\partial t}} + (\nabla.H_0 + \nabla.H_1) + \frac{\partial \overline{(K_M + \overline{V}V')\omega}}{\partial P} = -\overline{V}.\nabla\overline{\phi} - C(K_M, K_T) + \overline{V}.\overline{F} \qquad (1)$$

where

$$K_M = \frac{\overline{V}^2}{2} = \frac{\overline{V}.\overline{V}}{2}$$

mean kinetic energy

$$H_0 = K_M\overline{V}$$

$$H_1 = \overline{(\overline{V}.V')V'}$$

$$C(K_M, K_T) = C_H(K_M, K_T) + C_V(K_M, K_T)$$

$$C_H(K_M, K_T) = -\frac{\overline{u'u'}}{a\cos\varphi}\frac{\partial\overline{u}}{\partial\lambda} - \frac{\overline{u'v'}\cos\varphi}{a}\frac{\partial}{\partial\varphi} \times \left(\frac{\overline{u}}{a\cos\varphi}\right) - \frac{\overline{u'v'}}{a\cos\varphi}\frac{\partial\overline{v}}{\partial\lambda} - \frac{\overline{v'v'}}{a}\frac{\partial\overline{v}}{\partial\varphi} - \frac{\overline{u'u'v}\tan\varphi}{a}$$

$$C_V(K_M, K_T) = -\overline{u'\omega'}\frac{\partial\overline{u}}{\partial P} - \overline{v'\omega'}\frac{\partial\overline{v}}{\partial P}$$

The first term on the left hand side of Eq. (1) designates local rate of change of kinetic energy. The second and third terms describe horizontal and vertical divergence fluxes of kinetic energy respectively. Similarly, on the right hand side, the first term indicates adiabatic production of kinetic energy and the second term the exchange of energy between mean flow and the transients through the action of Reynold's stresses. The last term denotes the dissipation of kinetic energy by the turbulent frictional processes.

2.2 Mean Vorticity Budget Equation

$$\overline{\frac{\partial\zeta}{\partial t}} + \nabla.(\overline{\zeta} + f)\overline{V} + \frac{\partial(\overline{\zeta}\overline{\omega})}{\partial P} = -(\overline{\zeta} + f)\overline{D} - K.\nabla\overline{\omega} \times \frac{\partial\overline{V}}{\partial P} + Z \qquad (2)$$

where ζ is the relative vorticity, f is the Coriolis parameter, D is the horizontal divergence and Z is the residual of vorticity usually considered as an apparent vorticity source/sink. In the Eq. (2). first term on the left hand side designates the local rate of change of relative voriticty. The second and third terms represent the horizontal and vertical divergence fluxes of absolute vorticity and relative vorticity respectively. The first and second terms on the right hand side evince the production of vorticity through the stretching of vortex tubes and the tilting of isobaric surfaces respectively.

2.3 Mean Angular Momentum Budget Equation

$$\overline{\frac{\partial M}{\partial t}} + \nabla.\overline{V}\,\overline{M} + \frac{\partial}{\partial P}(\overline{\omega}\overline{M}) - fa\,\overline{v}\cos\varphi = -\frac{\partial\overline{\phi}}{\partial\lambda} + \delta\overline{\phi} + \overline{F}_\lambda \qquad (3)$$

where

$$M = u\,\overline{a}\cos\varphi$$

In the Eq. (3), the first term on the left hand side designates the time rate of change of momentum. The second, third and fourth terms describe the horizontal flux of relative momentum, vertical flux of relative momentum and the horizontal flux of Ω-momentum respectively. In the same manner, the first term on the right hand side

connotes the east-west pressure gradient. The second term indicates the generation/destruction of momentum due to mountain torque, and the last term describes the residue of momentum.

In the budget equations, the terms representing local rate of change of kinetic energy, relative vorticity and angular momentum over a period of 92 days (JJA) have negligible contribution towards the respective budgets. The results at each 1.5° regular latitude/longitude grid points are averaged both in zonal and meridional direction over the summer monsoon domain and integrated vertically from 1000 to 100 hPa. The volume integrations of the budget equations with the boundary conditions that ω vanishes at the bottom and the top of the atmosphere leads to elimination of all terms representing vertical flux divergence of various quantities. The last terms on the right hand side of the budget Eqs. (1)–(3) represent contributions from the sub grid scale processes. These terms are evaluated implicitly as residues of all the other terms in the respective budget equations.

3. Results and Discussion

In this study, all terms in various budget equations are evaluated over the summer monsoon region. Nevertheless, the discussion is confined to those which contribute significantly to the maintenance of the summer monsoon circulation. The flow characteristics in the forecasts of the NCMRWF are examined in the following section. The analysis of kinetic energy, vorticity and angular momentum budgets is presented in the subsequent sections.

3.1 Flow Characteristics

Distribution of vector wind fields in respect of mean analysis, forecast errors at day 1, day 3 and day 5 for 850 and 200 hPa pressure levels are presented in Figs. 1 and 2 respectively. The quasi permanent circulation features associated with the summer monsoon circulation are well depicted in the mean analysis and forecasts. The prominent monsoon circulation features of these two levels namely the low level Somali jet and the

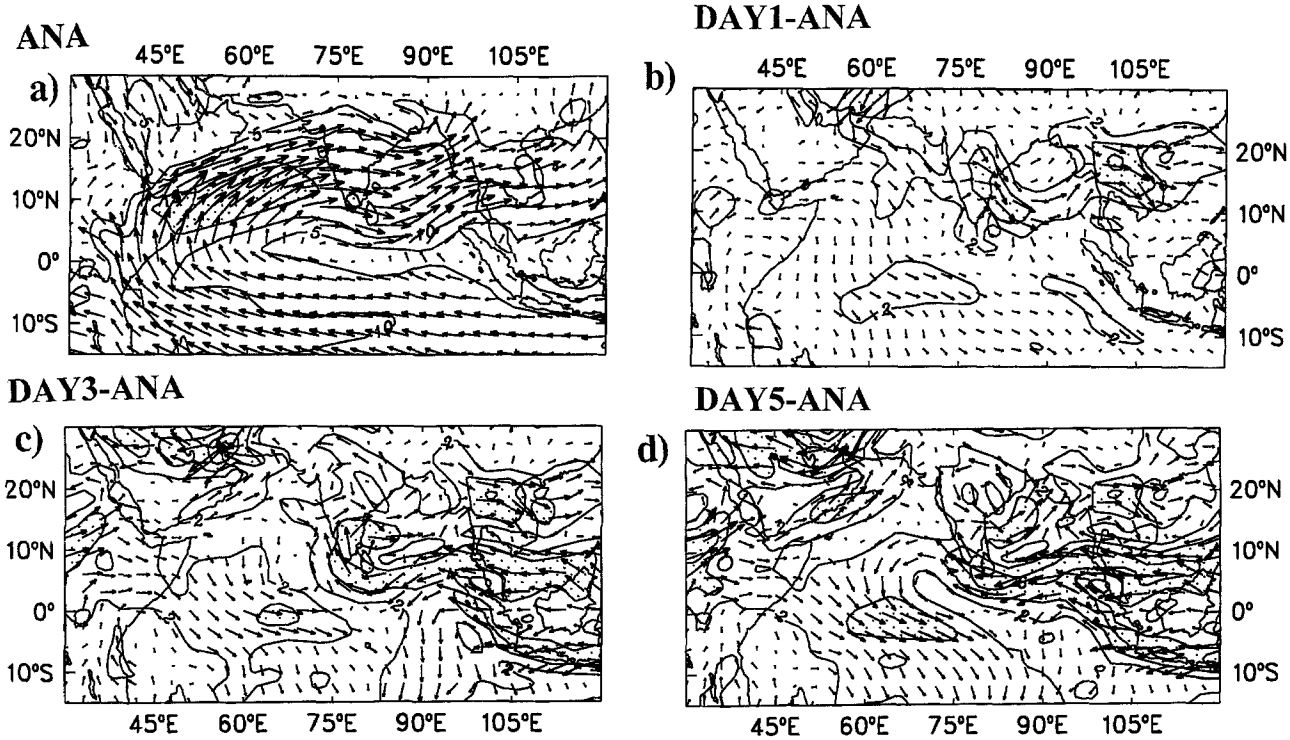

Fig. 1. Wind field at 850 hPa for JJA 1994 (a) Analysis (b) Day 1 forecast error (c) Day 3 forecast error (d) Day 5 forecast error [for a) contour interval: 5 ms^{-1}, wind field larger than 15 ms^{-1} is shaded; for b), c) and d) contour interval: 2 ms^{-1}; errors larger than 4 ms^{-1} are shaded]

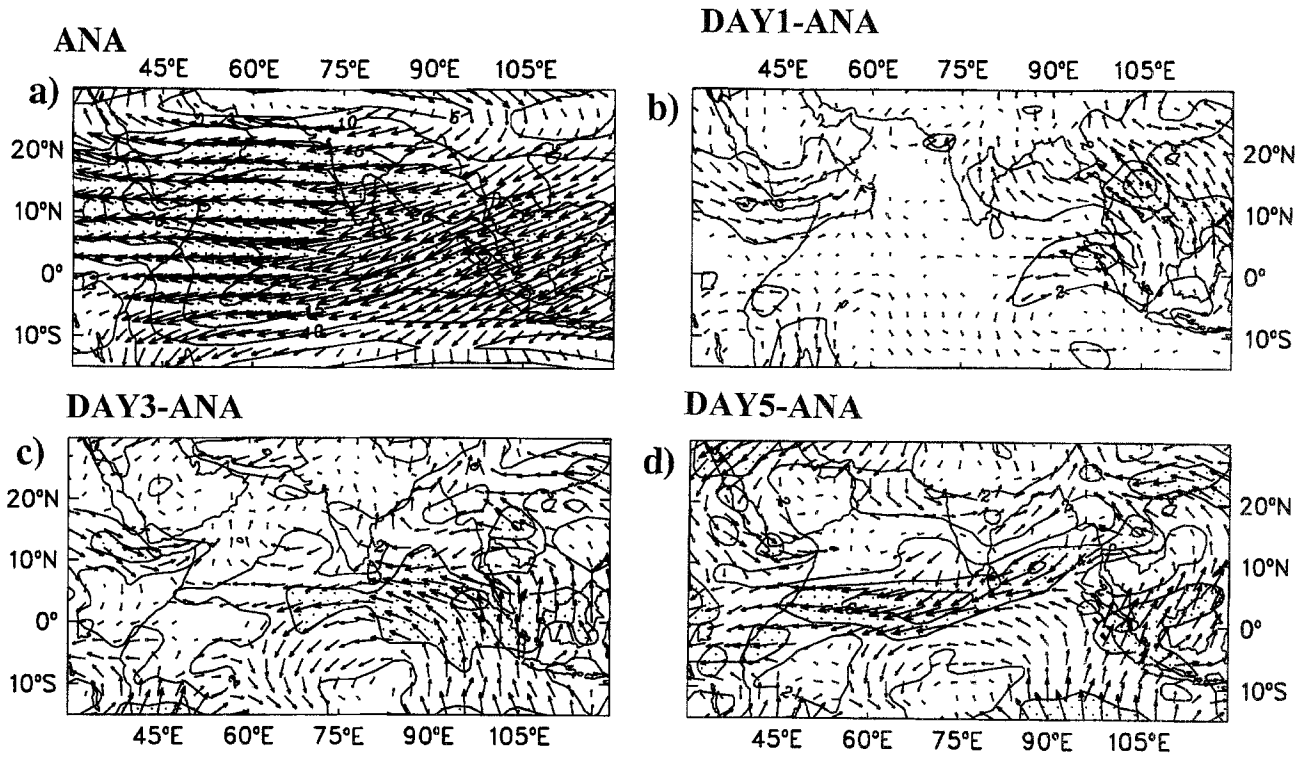

Fig. 2. Same as Fig. 1, but at 200 hPa

upper level strong Tropical Easterly Jet (TEJ) are in well agreement with their respective climatological features (Mohanty and Ramesh, 1994). The distribution of mean wind field of analysis at 850 hPa (Fig. 1a) depicts the existence of strong Southern Hemispheric trades having a speed of about 10 ms^{-1} (40° E–105° E), cross-equatorial flow into the Northern Hemisphere off the Somali coast and a zone of westerlies over the Arabian Sea and the Bay of Bengal (10–20 ms^{-1}).

In the course of model integration, flow characteristics at 850 hPa in the forecasts are dominated by generation of anomalous circulation (difference between forecast and analysis fields) features. A cyclonic circulation over the Bay of Bengal and an anti-cyclonic circulation over the Somali coast found to grow from day 1 through day 5. These anomalous features beget i) weakening of south easterly trades and the cross-equatorial flow (2–4 ms^{-1}) into the Northern Hemisphere; ii) intensification of westerly flow (2 ms^{-1}) to the north of 10° N and decreases to the south of it.

Wind field distribution at 200 hPa (Fig. 2a) is characterized by an intense and elongated anti-cyclone centered over Tibet (30° N) in the Northern Hemisphere. Two contrasting wind regimes present on either side of the Tibetan anti-cyclone, i.e. westerly wind regime (Sub-Tropical Jet) towards the north (not shown in Fig. 2a) and easterly regime to the south are the significant circulation features of the summer monsoon. Figure. 2a depicts a strong zone of easterlies which extends over Indonesia, Bay of Bengal, Arabian Sea and Africa with a core of maximum wind of 20 ms^{-1} around 9–12° N over the south Indian peninsula and adjoining Arabian Sea.

Analysis of the upper level flow characteristics reveal that the forecast errors are largely generated due to development of several anomalous circulation features (three anti-cyclones respectively over the Bay of Bengal, Arabian Sea and central regions (80° E–100° E) of South Indian Ocean) in the course of model integration. Further, a cyclonic circulation over Tibetan region particularly in day 3 and day 5 forecasts. These anomalous circulation features lead to (i) weakening of the Tibetan anti-cyclone, (ii) reduction of return flow into the Southern Hemisphere and (iii) intensification of easterly core over the North Indian Ocean (5–7 ms^{-1} by

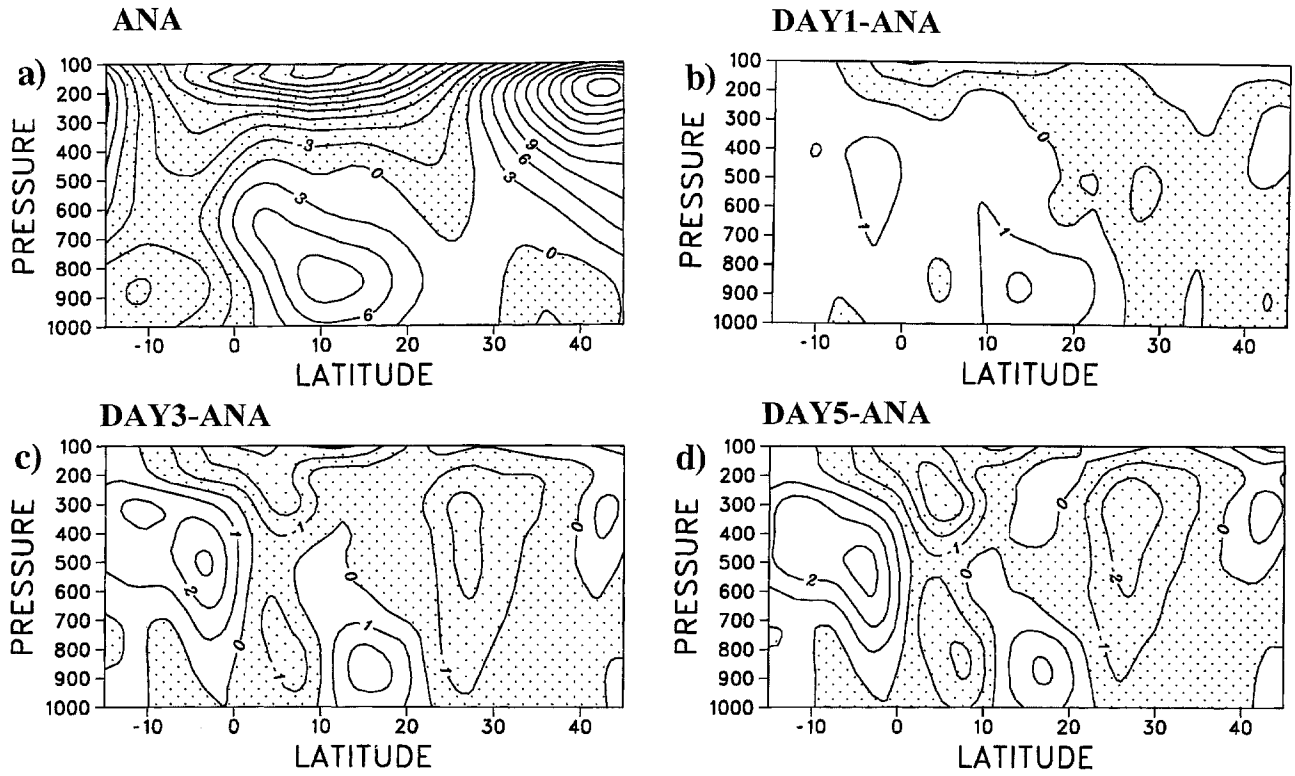

Fig. 3. Sectoral mean (30° E–120° E) pressure-latitude cross sections of zonal wind for JJA 1994. [units: ms^{-1}]. (a) Analysis (b) Day 1 forecast error (c) Day 3 forecast error (d) Day 5 forecast error [contour interval for (a): 3; for (b), (c) and (d): 1, negative values are shaded]

day-5). The overall effect of these errors indicates weakening of monsoon circulation with increase in the forecast period (up to day 5).

Generally, the summer monsoon is visualized as large scale convergence of mass and moisture over the Indian sub-continent and adjoining south east Asian land mass in the lower levels and a strong divergence in the upper levels. In order to examine the dominant characteristics of the monsoon circulation in the vertical plane, the sectoral (30° E–120° E) mean vertical cross sections of mean analyzed zonal wind and forecast errors (day 1-day 5) are presented in Fig. 3. The general pattern of the zonal wind in the monsoon region essentially consists of a low level maximum of westerly wind and an upper level maximum of easterly wind. Apparently, the monsoon westerlies in the lower troposphere of the Northern Hemisphere and easterlies in the lower troposphere of the Southern Hemisphere are well captured in the analysis. While the Sub Tropical Jet (STJ) core is well maintained, the zone of westerly flow to the south of STJ is found to be weakening in the medium range forecasts. However, the strength of low level monsoon westerlies increases to the north of 10° N and decreases to the south of it as the forecast period increases. The TEJ appears to intensify over the equatorial Indian Ocean in the forecasts (up to day 5). Further, the forecasts depict considerable weakening of the easterlies in the lower and middle tropospheres of the Southern Hemisphere.

The sectoral (30° E–120° E) mean of omega is illustrated in Fig. 4. Analysis delineates predominant rising motion except between 10° S–10° N and 30° N–35° N, where subsidence is noticed. The rising motion depicts two maxima over the monsoon region. The primary one around 700 hPa and the secondary around 500 hPa. The forecasts fairly simulate these features. However, day 3 forecast depicts increase in the subsidence zone between 10° S–10° N and decrease in the subsidence zone between 30° N–35° N. These subsidence zones persist in day-5 forecasts as well. The equatorial zone of decent is surrounded by zones of ascent on either side associated respectively with the Southern Hemispheric equatorial trough (SHET) to the south and with the Northern Hemispheric equatorial trough (NHET)/monsoon trough (MT)

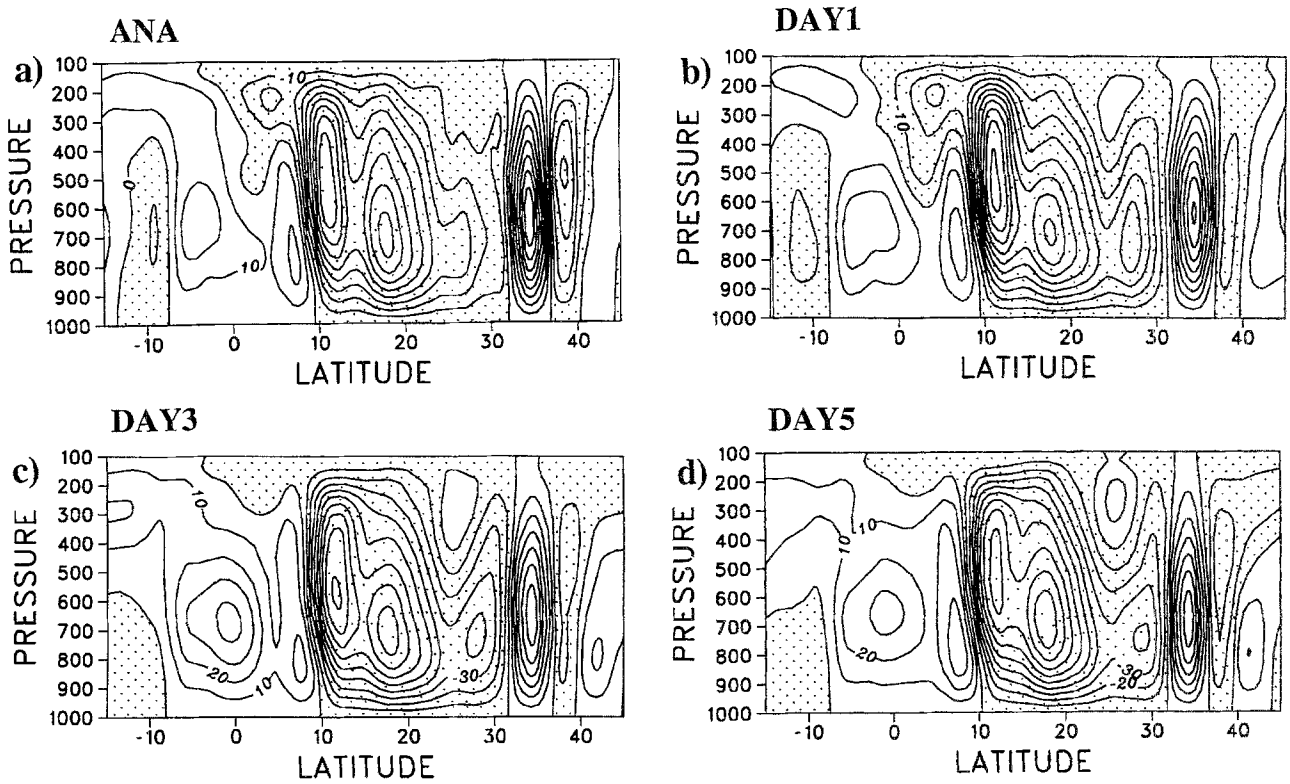

Fig. 4. Same as Fig. 3, but for omega [units: 10^{-3} Pa s^{-1}]. (a) Analysis (b) Day 1 forecast (c) Day 3 forecast (d) Day 5 forecast [control interval: 40, negative values are shaded]

to the north. It is interesting to note that the amplification of ascent in the forecast fields associated with NHET/MT is found to be associated with the weakening of the SHET.

The sectoral mean of relative vorticity field is presented in Fig. 5. It could be seen that the monsoon region is characterized by cyclonic (positive) vorticity in the lower troposphere and anticyclonic (negative) vorticity in the upper troposphere. However, the equatorial belt and extratropics are characterized by anticyclonic vorticity in the lower troposphere and cyclonic vorticity in the upper troposphere. Day 3 forecasts depict an increase in the strength of positive vorticity in the monsoon region which persists in day 5 as well. The increase in the strength is mainly due to intensification of westerlies over the north Bay of Bengal and development of anomalous cyclonic circulation over the south east Indian peninsula.

3.2 Kinetic Energy Budget

The maintenance of atmospheric general circulation is largely balanced by kinetic energy generation and dissipation. The generation of kinetic energy is manifested through conversion of available potential energy and dissipated through irreversible frictional processes. The local balance of kinetic energy is governed by three terms viz. the horizontal flux divergence, the adiabatic generation and the dissipation (through sub-grid scale frictional processes). The adiabatic generation of kinetic energy can be bifurcated in terms of its components namely zonal and meridional adiabatic generations. Also the mean flow kinetic energy flux divergence can be bifurcated in terms of its components and designated as

$$\nabla H = \nabla H_0 + \nabla H_1$$

The first term on the right hand side represents the flux transport of kinetic energy by the mean flow and the second term illustrates the mean transport of kinetic energy by the transient eddy motion. In the time mean horizontal flux of kinetic energy, the relative magnitudes of the flux transport by eddy flow are smaller compared to mean flow over the monsoon region.

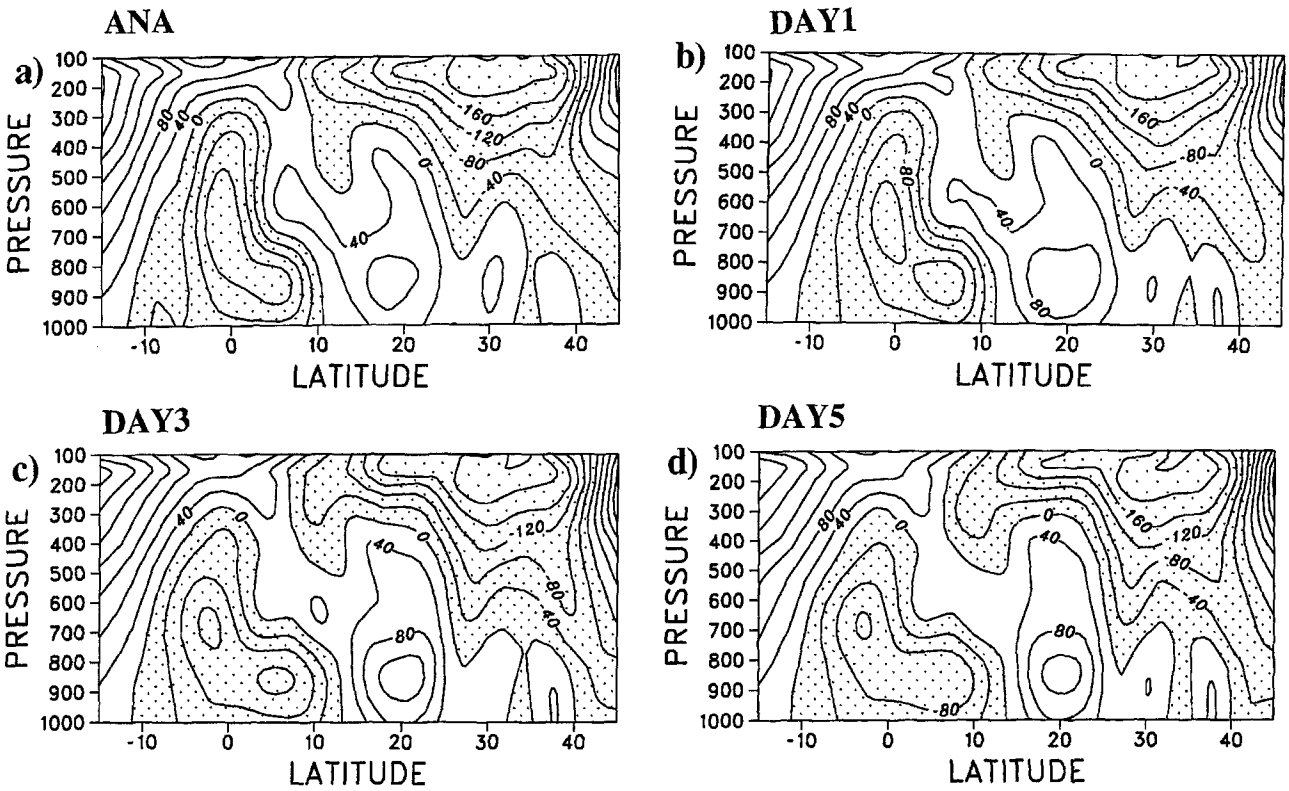

Fig. 5. Same as Fig. 3, but for vorticity [units $10^{-7}\,s^{-1}$]. (a) Analysis (b) Day 1 forecast (c) Day 3 forecast (d) Day 5 forecast [contour interval: 40, negative values are shaded]

The vertical profile of spatially averaged (15° S–45° N and 30° E–120° E), kinetic energy budget terms are presented in Fig. 6. The vertical profiles of the horizontal fluxes due to mean and eddy flows are represented in the Fig. 6a and 6b. In the lower and middle troposphere, the forecasts fairly represent the horizontal flux components. The mean component of the horizontal flux depicts weak flux convergence in the lower levels and strong flux divergence in the upper levels. However, the forecasts underestimate the flux divergence and depict strong flux convergence in the upper troposphere between 400–200 hPa levels. This may be due to the shrinking of zone of easterlies by the model in the troposphere between 500–300 hPa. The flux of KE due to mean flow is overestimated in day 5. This is due to increase of strong easterly bias ($6\,ms^{-1}$) over equatorial north Indian ocean and westerly bias over the west Pacific developing by day 5 in the course of model integration. These errors are moderate during day-1 and day 3 forecasts. In the case of eddy component also the forecasts underestimate the flux divergence in the upper troposphere. However, by day 5 the model could retain most of the analyzed divergence. The horizontal flux patterns depicted for the monsoon region are in good agreement with the earlier studies (Kung, 1966; Savijarvi, 1980, 1981). It was found that the source regions of kinetic energy are characterized by the strong flux divergence in the upper levels and convergence in the lower levels. The horizontal flux of kinetic energy characterizes the monsoon domain as the source region of kinetic energy.

The adiabatic generation of kinetic energy (Fig. 6c) shows two maxima, with a primary in the boundary layer and secondary in the upper troposphere (jet level). This aspect of generation of kinetic energy confirms several studies (Kung, 1966; Savijarvi, 1980, 1981). The zone of KE production in the planetary boundary layer over the Northern Hemisphere is confined to tropics indicating the presence of strong ageostrophic flow. Since, Kung and Savijarvi carried out the budget estimations over the north American region the one-to-one correspondence may not be possible. The forecasts fairly represent the

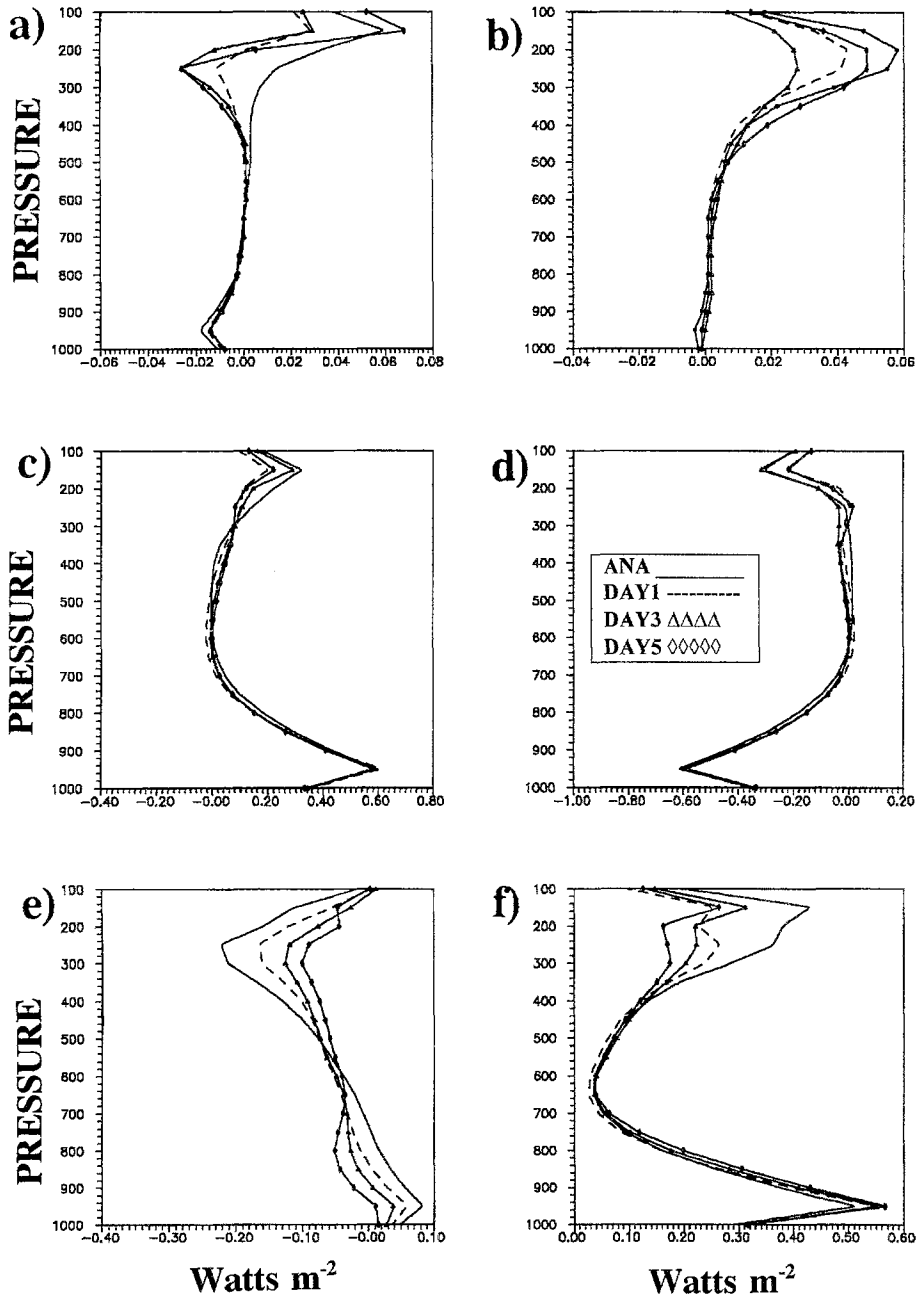

Fig. 6. Vertical profile of kinetic energy budget terms for JJA 1994. (a) horizontal flux of kinetic energy due to mean component of flow (b) horizontal flux of kinetic energy due to eddy component of flow (c) adiabatic generation of kinetic energy (d) dissipation of kinetic energy (e) zonal adiabatic generation of kinetic energy (f) meridional adiabatic generation of kinetic energy

generation of kinetic energy in the lower troposphere, but underestimates in the upper troposphere at the jet level. The diabatic dissipation of kinetic energy budget balances the production. It is estimated as the residue implicitly. The residue is parametrized through turbulent momentum fluxes with the aid of surface similarity and mixing length theories in the forecast model. The residue of KE also shows two maxima, the primary in the boundary layer and the secondary in the free atmosphere at upper levels (Kung, 1966) associated with TEJ and STJ (Fig. 6d). The boundary layer dissipation values in the observed data studies (Kung and Baker, 1975; Holopainen and Eerola 1979) are close to those over the monsoon region. The boundary layer dissipation values for the three regions namely North America, North Atlantic and Europe for summer season computed by Savijarvi (1981) with the ECMWF analyses are given in the Table 1 for comparison with those of the Asian summer monsoon (ASM) region.

Table 1. *Comparison of Boudary Layer (below 850 hPa) Dissipation from ECMWF Analysis (Wm^{-2}) [from Savijarvi, 1981] with NCMRWF Analysis & Forecasts for Asian Monsoon Region (ASM)*

Region	Boundary layer dissipation (Wm^{-2})
North America*	1.0
North Atlantic*	1.2
Europe*	1.4
ASM Analysis	1.65
ASM Day 1 forecasts	1.68
ASM Day 3 forecasts	1.64
ASM Day 5 forecasts	1.61

* Results from Savijari, 1981 with the ECMWF analysis are reproduced for comparison purpose.

The magnitudes depicted in Table 1 shows that the simulated boundary layer dissipation over ASM region are comparable but marginally higher than the corresponding values of other regions due to stronger low-level flow associated with ASM. Although the adiabatic generation is the resultant of zonal and meridional ageostrophic components, the contributions from the meridional component is significant (the zonal component is one order less than that of meridional component). The zonal and meridional components of the adiabatic generation are represented in Fig. 6e and 6f respectively. The zonal adiabatic generation is underestimated in lower as well as higher levels and such tendency is found to increase with increase in the forecast period. This is due to weakening of the zonal flow of the monsoon circulation over the Arabian Sea with increase in the forecast period. However, the meridional component depicts the lower level generation fairly well and weaker generation in the upper levels. While the strong generation in the lower levels is enabled through meridional ageostrophic component, the weak return flow in the upper levels contributes to its underestimation in the upper levels.

Vertically integrated (1000–100 hPa) geographical distributions of horizontal flux of kinetic energy (for the analysis and forecast fields) are presented in Fig. 7. A dominant flux divergence regime of kinetic energy which extends all over the south Asian region from Western Pacific to East Africa (with flux divergence maxima over the Bay of Bengal and eastern Arabian Sea) is

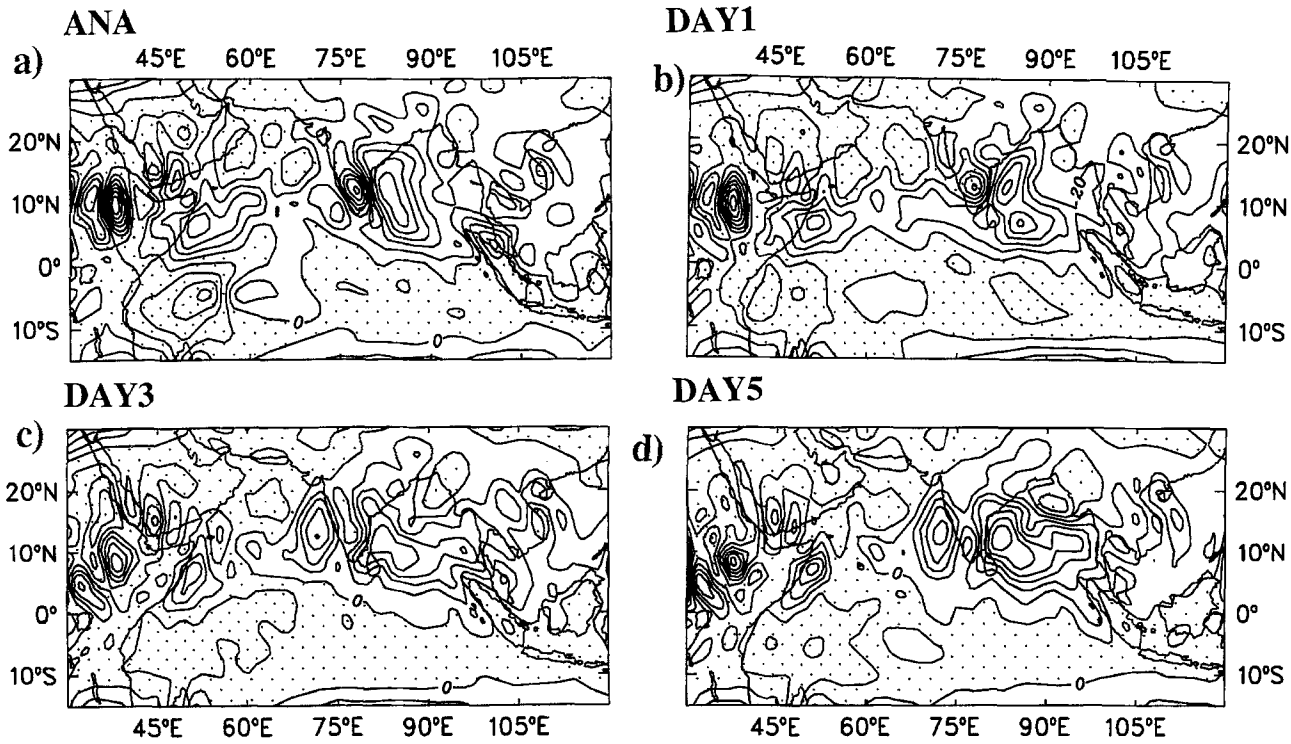

Fig. 7. Geographical distribution of vertically integrated horizontal flux of kinetic energy for JJA 1994. [units: 10^{-1} Watts m^{-2}]. (a) Analysis (b) Day 1 forecast (c) Day 3 forecast (d) Day 5 forecast. [contour interval: 20, negative values are shaded.]

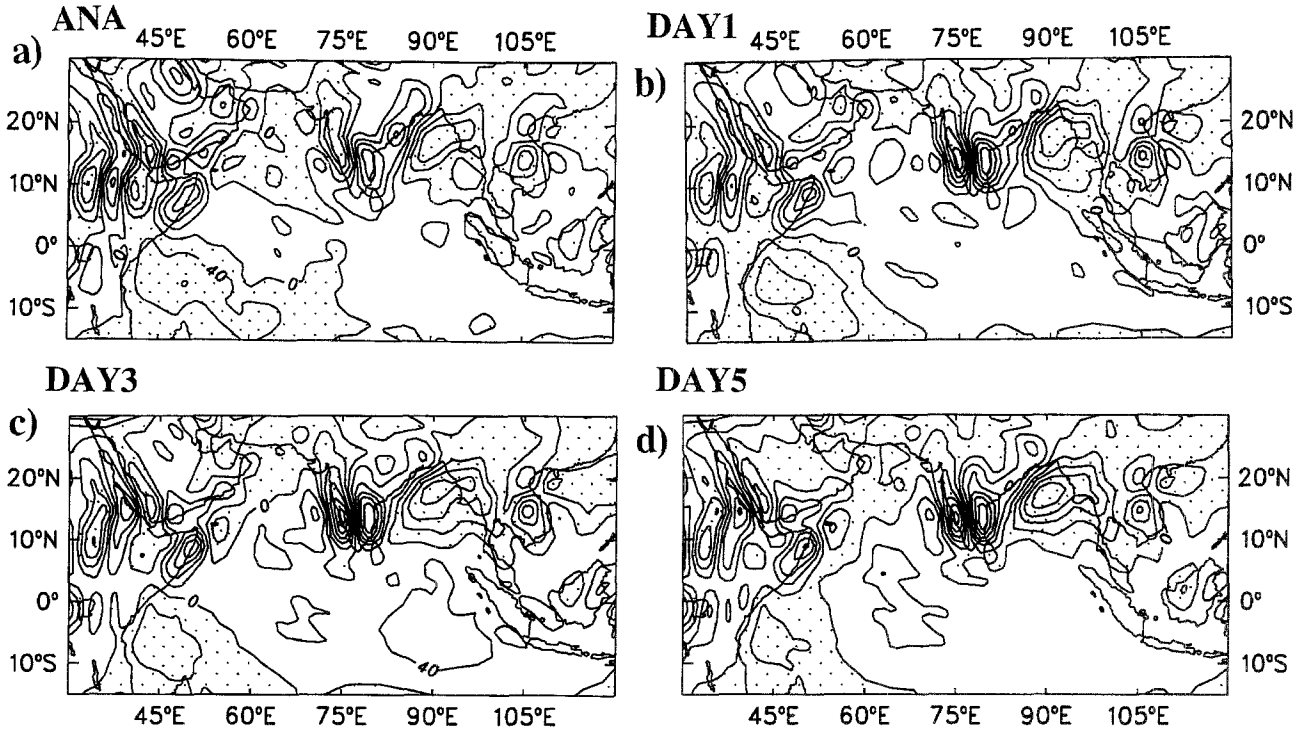

Fig. 8. Same as Fig. 7, but for zonal adiabatic generation of kinetic energy. [contour interval: 40, negative values are shaded]

noticed. The kinetic energy flux convergence is observed over the northwest Arabian Sea, adjoining Arabia, North Africa and Equatorial Indian Ocean off East Africa and peninsular Indian. These zones of kinetic energy flux transport maxima/minima are situated at the respective locations of entrance/exit regions of the tropical easterly jet. All these features are well captured in the forecasts which are in conformity with earlier studies (Mohanty and Ramesh, 1994) carried out with the ECMWF analyses. The model forecasts indicates the presence of a relatively weaker zone of flux divergence over the west Bay of Bengal compared to that of analysis and a gradual spreading of the zone of flux divergence into the eastern sector of Bay of Bengal in the forecast fields. On the otherhand, the respective zones of KE flux convergence and divergence prevalent over the south Indian peninsula and eastern Arabian Sea are more or less maintained at the same level in day 1 forecasts (Fig. 7b). But day 3 and day 5 forecasts suggests strengthening of the flux divergence maxima of the Arabian Sea and weakening of the flux convergence maxima over the south peninsula and the west equatorial Indian Ocean. The increase in the Arabian Sea kinetic energy flux divergence maximum may be due to strong upper level (200 hPa) easterly bias displayed by the model from day 3. Similarly the intensity of the KE flux convergence zone located at the exit region of the TEJ over the west equatorial Indian Ocean is found to be weakening from day 1 to day 5 forecasts (Fig. 7a–d). The weakening of the flux convergence over the exit region of the TEJ is largely attributed to the weakening of the easterly flow over the region in the course of model integration upto day 5.

The generation of kinetic energy depends on the nature of ageostrophic motion in general. The positive values denote the production from the source of APE, while negative values denote its destruction i.e. return to the reservoir of APE and these processes are adiabatic (Lorenz, 1967). The vertically integrated zonal adiabatic generation of kinetic energy (Fig. 8) contributes for generation of kinetic energy over the east coast of the peninsular India, south eastern Arabian Sea and Somalia region of East Africa. A strong zone of kinetic energy destruction is noticed over Northeast Bay and adjoining Myanmar region. This is possibly due to the sub-geostrophic nature of the flow over these regions. A general correspondence between the adiabatic production (destruc-

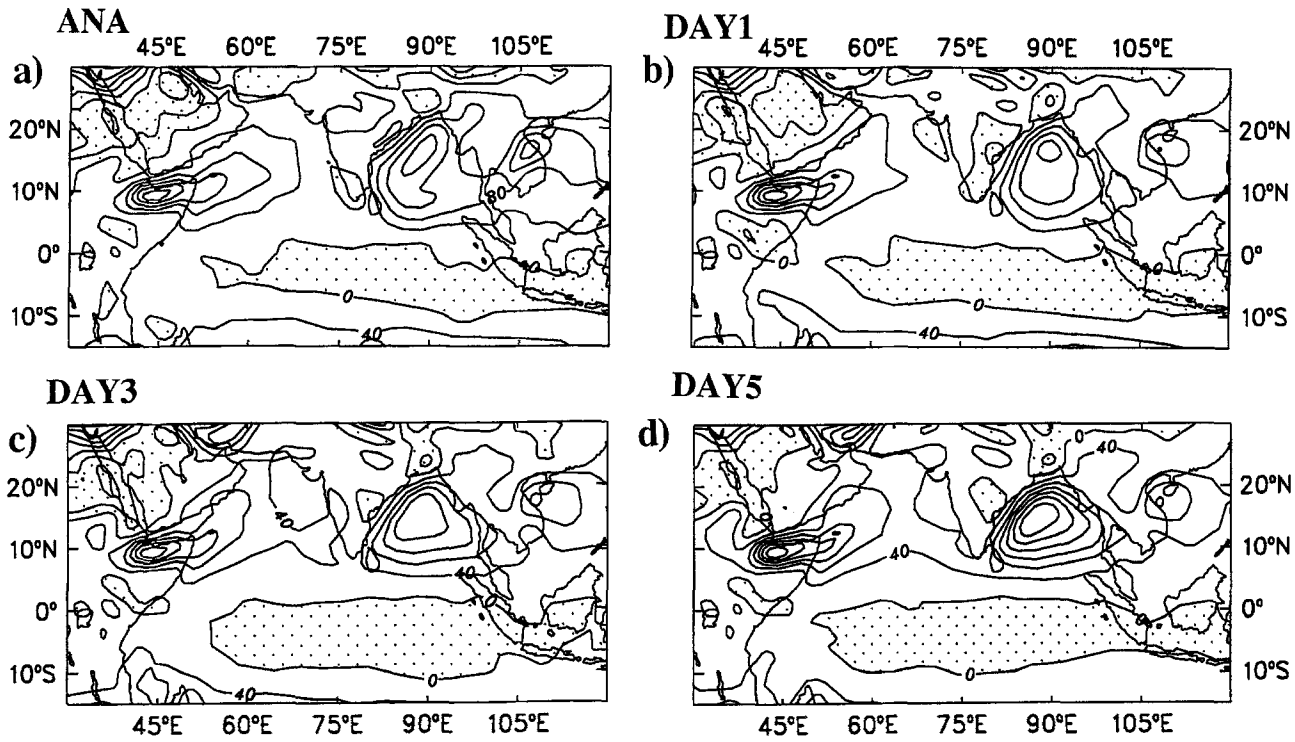

Fig. 9. Same as Fig. 7, but for meridional adiabatic generation of kinetic energy. [contour interval: 40; negative values are shaded]

tion) of kinetic energy and the super-geostrophic (sub-geostrophic) nature of the flow is demonstrated (Kung, 1971). The forecasts suggest that the corresponding maxima of production/destruction of KE are more or less simulated reasonably well with relatively strong zones of destruction maximum over the Bay of Bengal and generation maximum off East Africa and the Southeast Arabian Sea. The meridional generation of kinetic energy is depicted in Fig. 9. Except for some parts of eastern Arabian Sea, eastern peninsular India and equatorial Indian Ocean, the entire monsoon region is dominated by kinetic energy production with maxima over the Bay and Bengal and off East Africa respectively. Though, the meridional generation is well simulated, the forecasts underestimate the maxima over the Bay of Bengal and East Africa as the forecast period increases. It is found that over the Arabian Sea the seasonal mean distributions of zonal and meridional components of adiabatic generation of KE in the forecast fields differ from that of analyses (Figs. 8–9). Notable features which develop in the course of model integration include, weakening of the zonal component of adiabatic destruction over the Central Arabian Sea (Fig. 8) and the anomalous amplification of adiabatic production of meridional component of KE over the eastern Arabian Sea (Fig. 9). The presence of anomalous zones of kinetic energy production especially in day-3 and day-5 forecasts over the eastern Arabian Sea is mainly attributed to the anomalous flow characteristics with a growing tendency upto day-3 in correspondence with the vertical motion (Fig. 4).

In order to elucidate the representation of transient eddy circulations by the model over the Asian summer monsoon region, some of the eddy components of kinetic energy budget are depicted in Fig. 10. The sectoral mean kinetic energy horizontal flux due to eddy component of flow is illustrated in Fig. 10a and b for the analysis and day 5 forecast. The model forecasts clearly delineate the underestimation of transient circulations with the increase in forecast length. Nonetheless, the forecasts generally maintain the analyzed pattern. The eddy generation of kinetic energy (Fig. 10c and d) also depicts underestimation in the upper levels and slight overestimation in the lower levels. The marginal

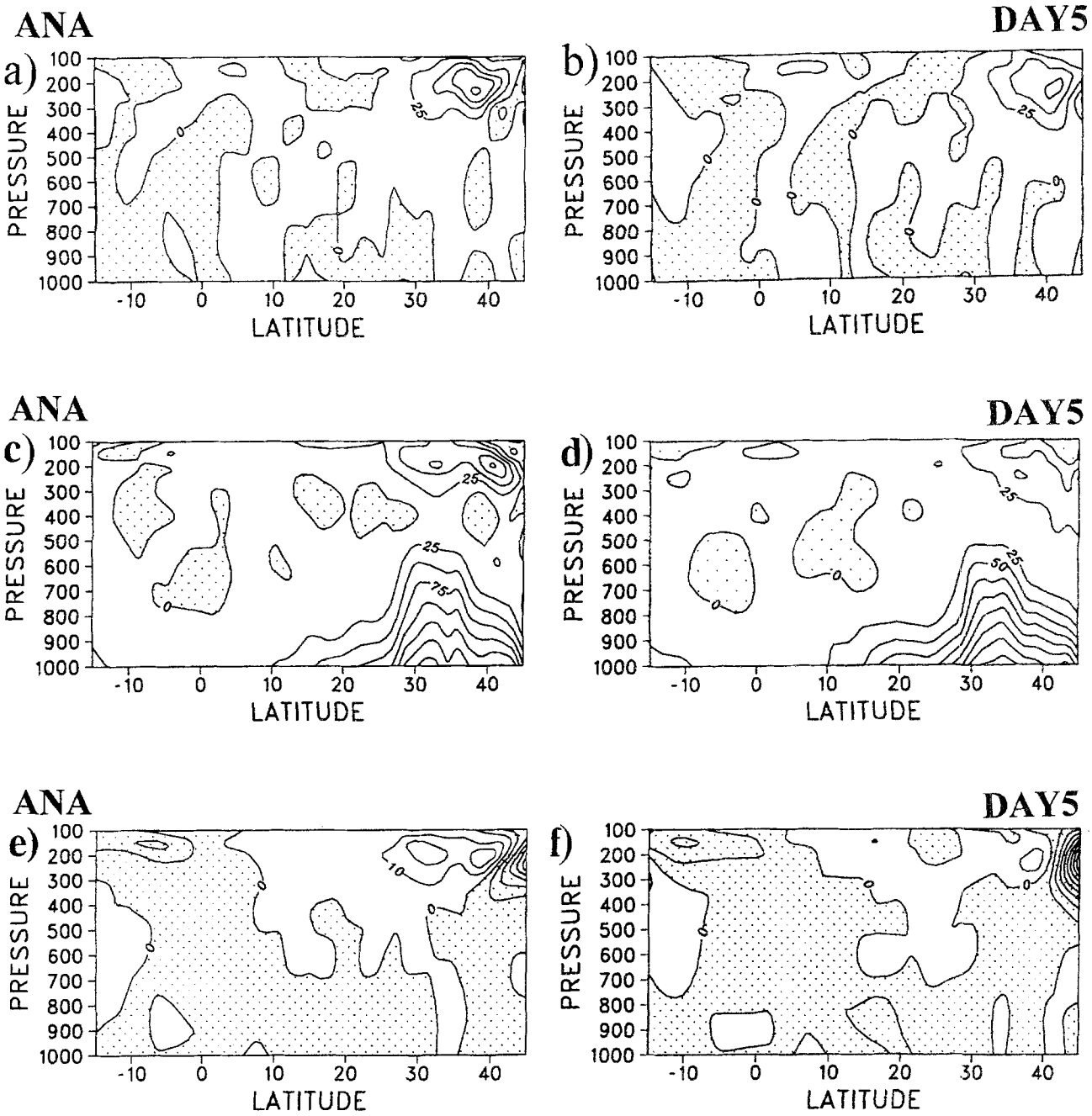

Fig. 10. Sectoral mean (30° E–120° E) pressure-latitude cross sections of eddy kinetic energy budget terms for JJA 1994 [units: 10^{-5} Watts kg^{-1}] (a) Analysis of horizontal flux due to eddy component of the flow (b) Day 5 forecast (c) and (d) same as (a) and (b); but for eddy generation of kinetic energy (e) and (f) same as (a) and (b); but for mean to eddy conversion of kinetic energy [contour interval for (a), (b), (c), & (d) : 25, for (e) & (f): 10, negative values are shaded]

strengthening in the lower level flow in the model during day 5 explains the lower level overestimation. However, the representation of mean orography in the model makes the underestimation of transients in general (White, 1988a). This offers the plausible reason for underestimation in the upper levels. Figure 10e and f shows the conversion of kinetic energy between the mean flow and the transients. Positive magnitudes denote mean to eddy conversion and negative magnitudes the vice versa. The forecasts fairly simulate the conversion term. However, day 5 forecast depicts substantial increase in the eddy to mean conversion north of 40° N in the upper tropo-

spheric levels and weakening of the mean to eddy conversion around 30° N.

It is evident from kinetic energy budget that the forecasts fail to maintain the analyzed atmospheric circulation characteristics. This is presumably explained by underestimation of both kind of eddies with periods associated with baroclinic eddies and eddies of lower frequencies. Experiments (White, 1988a) suggest that the use of mean as well as enhanced orography slightly decreases the strength of transient eddies. The gravity wave drag also to some extent dampen the transient eddies. However, studies (White, 1988b) carried out at NCEP also show the underestimation of transient eddies in the Southern Hemisphere. Hence the above two factors may be insufficient to explain the damping of transients. The effect of reducing horizontal diffusion (Alpert et al., 1988) reduces model's negative height bias and the impact of correcting negative height bias is to be studied. Further, the use of interactive clouds and the effect of the vertical diffusion need to be examined.

3.3 Vorticity Budget

The terms in the vorticity budget equation which contribute significantly to the budget are vorticity transport and generation due to stretching and tilting terms (Holopainen and Oort, 1981; Chu et al., 1981). However, in the vertically integrated domain of vorticity budget, the planetary vorticity advection and the relative vorticity advection terms largely govern the balance of vorticity.

The vertical profile of spatially averaged vorticity budget terms is presented in Fig. 11. The horizontal advection of relative vorticity depicts a maximum in the boundary layer around 950 hPa and minimum around 400 hPa. However, the horizontal advection of planetary vorticity denotes maximum at 950 hPa and minimum around 150 hPa. At other levels planetary vortic-

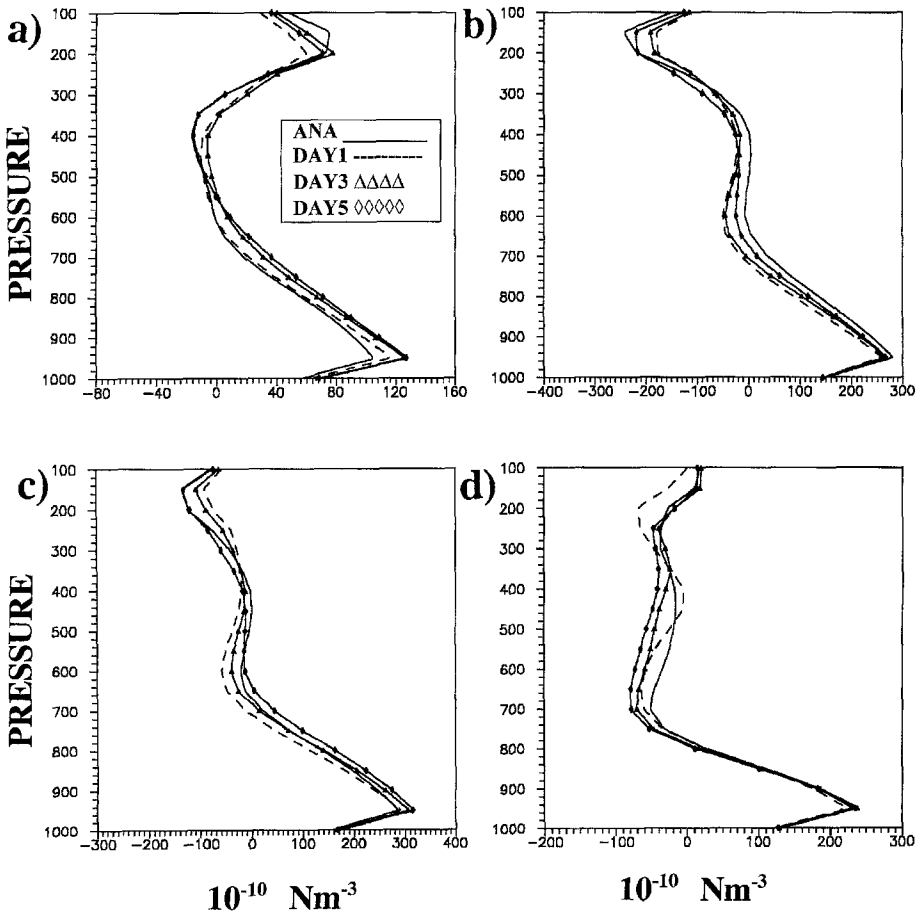

Fig. 11. Vertical profile of vorticity budget terms for JJA 1994. (a) horizontal advection of relative vorticity (b) horizontal advection of planetary vorticity (c) generation of vorticity due to stretching (d) residue of vorticity

ity shows negative advection and the relative vorticity indicates positive advection, and thus they balance each other. The forecasts depict overestimation of relative vorticity advection and underestimation of planetary vorticity advection. The increase in relative vorticity advection is due to intensification of westerlies north of 10° N over the Arabian Sea and the Bay of Bengal. The reduction tendency in the case of planetary vorticity is mainly due to decrease in the cross equatorial flow in the lower levels and the return flow in the upper levels. The monsoon circulation is maintained by excess generation of vorticity (due to stretching) in the lower levels. The vorticity generation reaches maximum in the boundary layer, minimum around 600 hPa and thereafter anti-cyclonic vorticity is generated. The generation of vorticity depicts the monsoon domain as the source region of vorticity. All forecasts illustrate this feature despite slight underestimation in the day-1 and day-3 forecasts. The vorticity residue (Fig. 11d) indicates the production/destruction of vorticity due to sub-grid scale processes. The analysis shows that the vorticity residue contributes for the generation in the lower troposphere and dissipation in the middle and upper troposphere. All forecasts represent the generation realistically, however, the destruction is slightly overestimated in the residue of vorticity in the middle and upper tropospheric levels in all ranges of forecasts. Earlier studies (Reed and Johnson, 1974; Chu et al., 1981) reveal that cumulus convection in the tropics generate apparent source of vorticity. In the monsoon domain, the sub-grid scale generation of vorticity is manifested through cumulus convection. The excessive destruction of vorticity in the forecasts, in the middle levels delineate the deficiencies in the representation of convection over the monsoon region.

The vertically integrated geographical distribution of the horizontal advection of relative vorticity is illustrated in Fig. 12. It is noticed that the monsoon domain is characterized by predominant horizontal advection of relative vorticity. The essential features such as zones of flux divergence surrounding southeast Arabian Sea and northwest Bay of Bengal regions are reproduced. Also, zones of flux convergence surrounding northeast sectors of the Arabian Sea

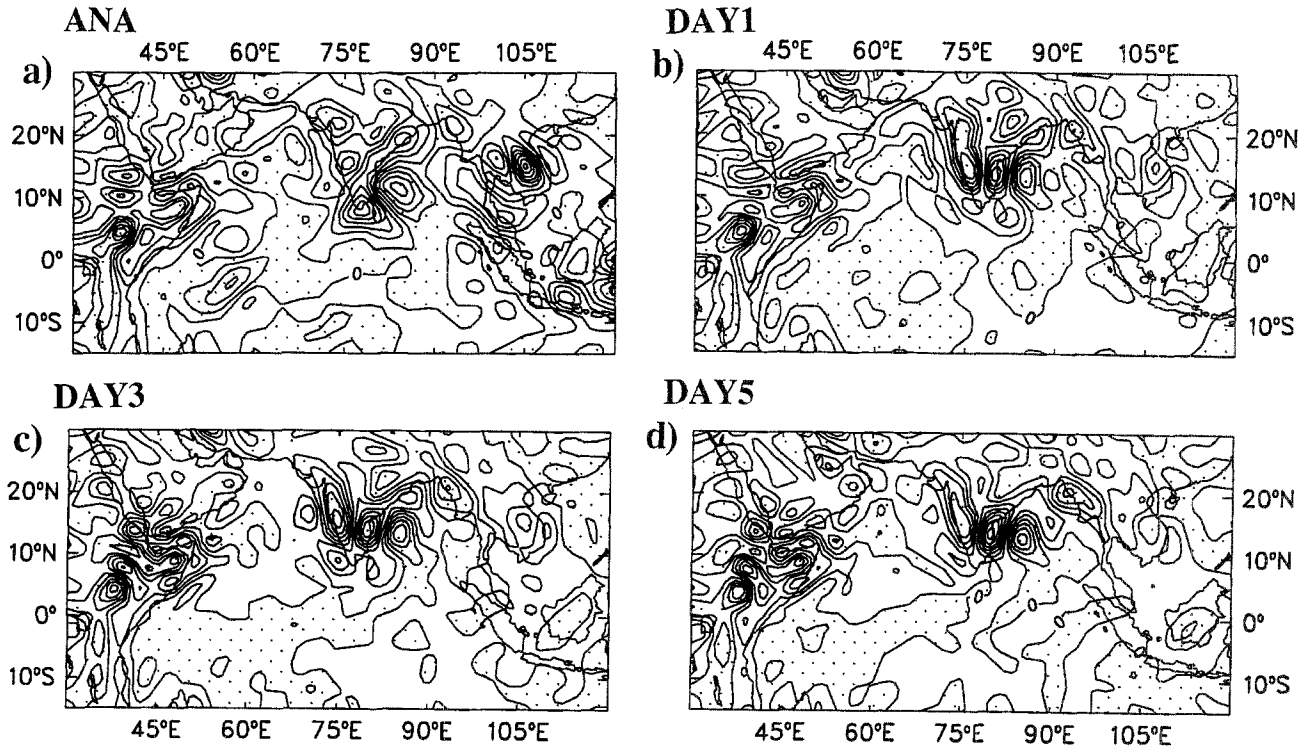

Fig. 12. Geographical distribution of vertically integrated horizontal advection of relative vorticity for JJA 1994. [units: 10^{-8} N m^{-3}] (a) Analysis (b) Day 1 forecast (c) Day 3 forecast (d) Day 5 forecast [contour interval: 50, negative values are shaded]

and Bay of Bengal are well represented in the analysis fields (Fig. 12a) although the relative strength is found to be stronger than the climatology (Mohanty and Ramesh, 1994). On the otherhand, the corresponding distributions of vertically integrated relative vorticity advection produced using the forecast fields (Fig. 12) suggest an anomalous increase in the flux divergence over the Southwest Bay of Bengal and adjoining south peninsula, flux convergence over the southwest peninsula and weakening of flux divergence over the southeast Arabian Sea.

The vertically integrated planetary vorticity advection is shown in Fig. 13. It could be seen that both of these vorticity advection terms (the planetary vorticity advection and the relative vorticity advection) oppose each other in the monsoon region. The planetary vorticity advection is found to be dominant over the Head Bay of Bengal, west Indian Ocean and the adjoining African continent. The presence of strong planetary vorticity advection off East Africa may be attributed to the anomalous features noticed in the lower tropospheric levels over the region (Fig. 13a). Over the eastern Arabian Sea and the Indian subcontinent a net convergence of vorticity is observed. Due to systematic biases of the model as discussed earlier, the increasing tendency in the flux divergence is noticed in the maximum of the Head Bay of Bengal and decreasing tendency in the maximum of East African coast as the forecast process advances. However, the convergence over Indian subcontinent is well brought out in the forecasts except in day 5 where slight amplification is noticed. The combined effect of these two terms contributes towards the net vorticity advection over the monsoon region. In view of the results discussed earlier, the same is atleast not true over the southeastern Arabian Sea for the forecasts (Figs. 12–13). In the Northern Hemispheric tropics the vorticity advection zones are supported by vorticity generation which is due to the presence of cyclonic circulation in association with the intense low level convergence. In the upper levels the stretching term contributes towards the generation of anti-cyclonic vorticity to the south of Tibetan high due to the presence of anti-cyclonic circulation in association with strong divergence.

In order to balance the net vorticity advection over the monsoon region, and thus to sustain the circulation, the generation of vorticity is imminent within the domain itself. The vertically

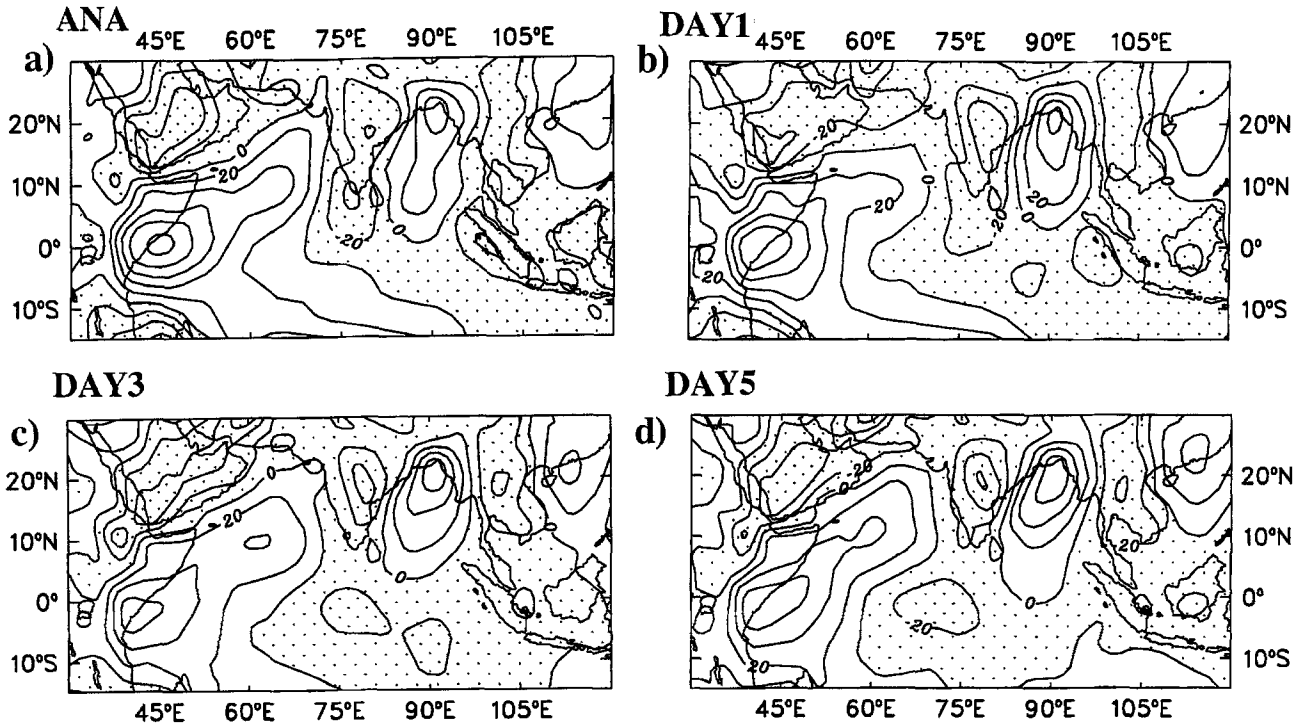

Fig. 13. Same as Fig. 12, but for horizontal advection of planetary vorticity [contour interval: 20, negative values are shaded]

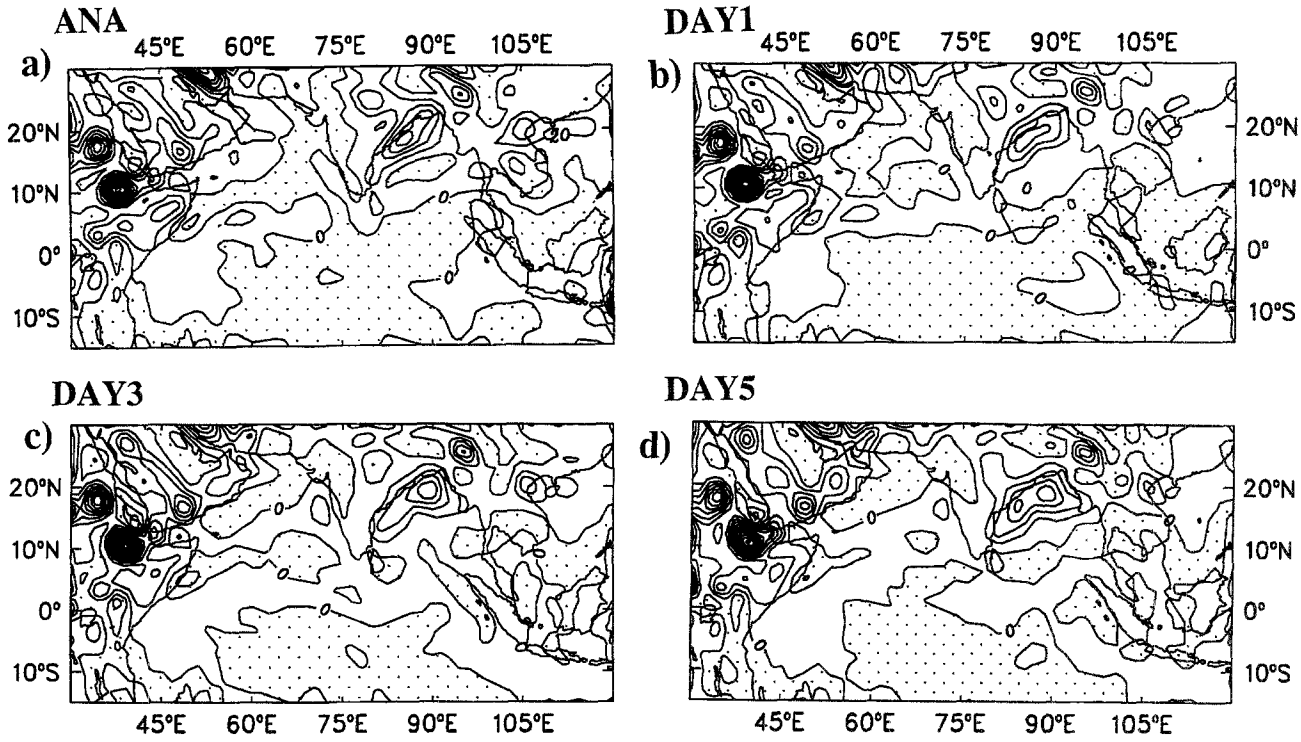

Fig. 14. Same as Fig. 12, but for generation of vorticity due to stretching. [contour interval : 20, negative values are shaded]

integrated vorticity generation due to stretching is depicted in Fig. 14. The generation of vorticity is noticed over most parts of Indian region and the Bay of Bengal with maximum over west central Bay of Bengal. Elsewhere weaker dissipation is noticed. The medium range forecasts fairly simulate the generation maximum over the Bay of Bengal. In general, the generation of vorticity is possibly due to the cyclonic shear associated with the monsoon trough over the Head Bay and movement of cyclonic vortices into the region from east and their subsequent intensification. Although the forecasts maintain the balance reasonably well, due to anomalous cyclonic circulation over the Bay of Bengal the relative vorticity advection is overestimated in day 3 and day 5 forecasts. Further, the forecasts underestimate planetary vorticity advection which is due to reduction of cross equatorial flow with increase in the forecast period.

The large scale balance of vorticity is governed by the horizontal transportation and the generation due to sub-grid scale processes, as the vorticity generated through stretching and tilting terms does not suffice to satisfy the balance requirements over the monsoon region. This supports earlier observations (Holton and Colton, 1972 and Fien, 1977) that the monsoon domain is characterized by generation of vorticity through subgrid scale processes such as cumulus convection. Furthermore, earlier studies (Reed and Johnson, 1974; Chu et al., 1981) confirm the fact that cumulus convection in the tropics could generate large apparent source of vorticity.

3.4 Angular Momentum Budget

The regional balance in the angular momentum budget is governed by the omega momentum flux, the pressure torque (or the east west pressure gradient) and the dissipation term (or the residue) of the angular momentum. The vertical profile of spatial averaged budget terms is depicted in Fig. 15.

The horizontal flux of omega momentum (Fig. 15a) indicates convergence in the lower troposphere upto 600 hPa and divergence in the upper troposphere upto 200 hPa. Although the forecasts captured these features fairly well, strong convergence in the lower levels during day 1 and weak divergence in the upper levels during day 5 are noticed. The vertical profile of relative angular momentum flux shows weak conver-

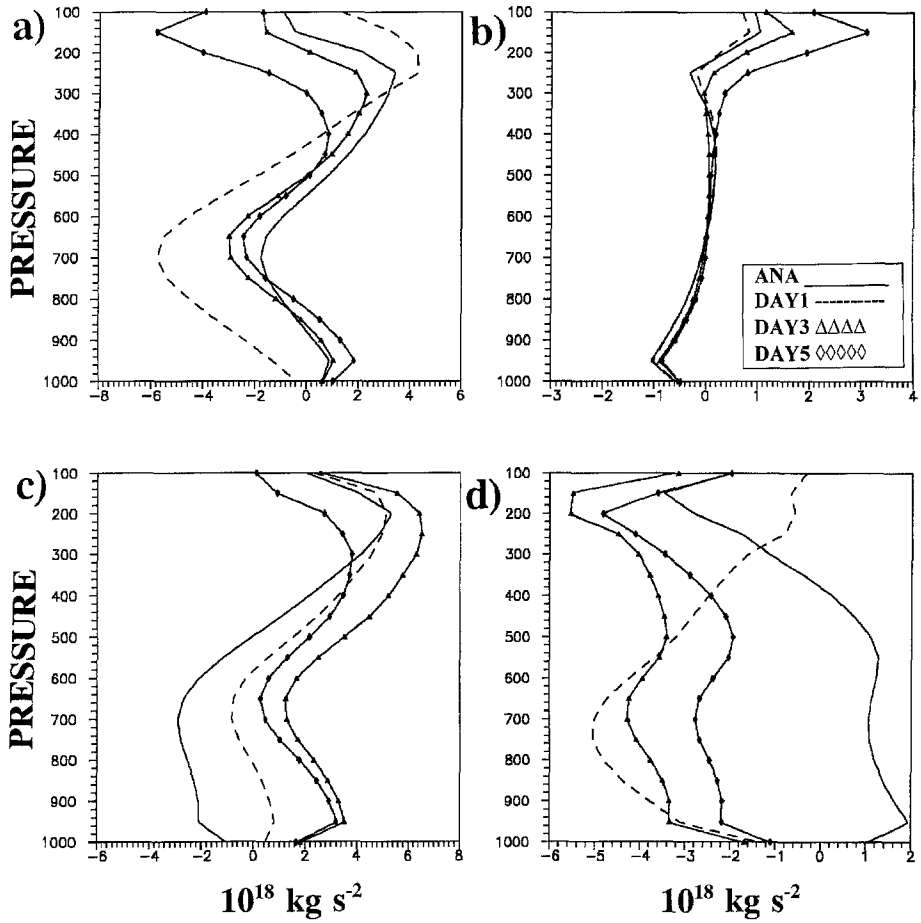

Fig. 15. Vertical profile of angular momentum budget terms for JJA 1994. (a) horizontal flux of omega momentum (b) horizontal flux of relative momentum (c) pressure torque (d) residue of angular momentum

gence in the lower levels and weak divergence in the upper levels. The forecasts fairly represent the relative angular momentum flux variation in the vertical. However, day 3 and day 5 forecasts show comparatively excess divergence in the upper levels. This is attributed to the systematic easterly bias of the model from day 3. As the variations of zonal wind determine the variations of the relative momentum, the increase in easterlies in the upper levels, influence the horizontal flux of relative momentum. The pressure torque contributes for the dissipation of momentum in the lower levels and generation in the upper levels. Although the forecasts depict same tendency, they underestimate the pressure torque due to which the model forecasts generate momentum in the monsoon region instead of its destruction. The medium range forecasts of the model evince systematic negative height bias increasing with height. The pressure torque is underestimated due to this error.

The residue of angular momentum (Fig. 15d) shows generation of angular momentum in the lower levels and dissipation in the upper levels. The forecasts fail to simulate these features due to negative height bias of the model. All forecasts indicate dissipation throughout the troposphere. However, day 1 forecast shows excessive dissipation in the lower level and less in the upper levels. Since horizontal flux of omega momentum and pressure torque are the principle contributors to the residue of angular momentum, the errors crept into them reflected here also. The errors in those fields are marginally lower during day 3 and day 5.

The angular momentum balance is further elucidated through vertically integrated budget terms. The horizontal flux of omega momentum is shown in Fig. 16. Analysis indicates flux divergence over Indian subcontinent, Arabia and Myanmar regions and flux convergence over South East China, the Bay of Bengal, the Arabian Sea and parts of South Indian Ocean. The model forecasts brought out these aspects fairly well, except overestimating the convergence slightly. It is noticed that the convergence maxima are

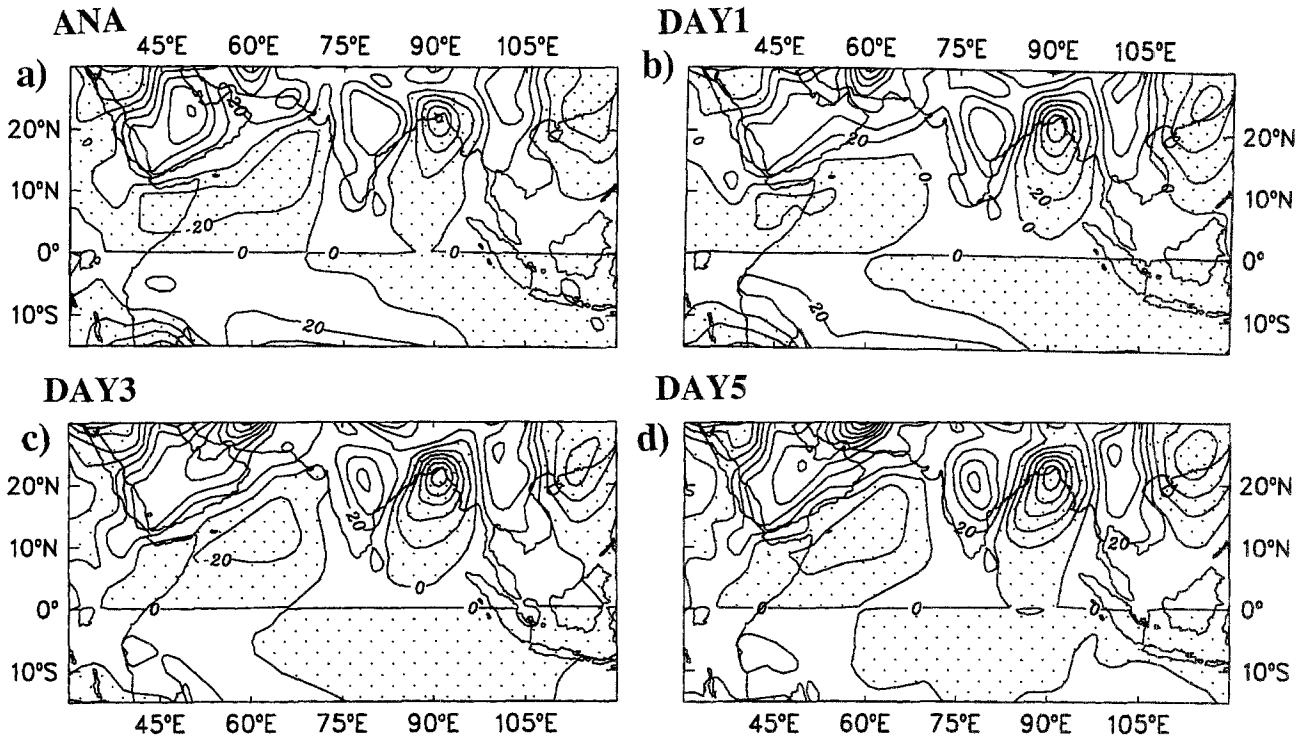

Fig. 16. Geographical distribution of vertically integrated horizontal flux of omega momentum flux for JJA 1994. [units: $10^5\,kg\,s^{-2}$] (a) Analysis (b) Day 1 forecast (c) Day 3 forecast (d) Day 5 forecast [contour interval: 20, negative values are shaded.]

located over the cyclogenetic area of North Bay of Bengal and South China Sea and divergence maxima over the heat low which extends right from Arabia to India.

The pressure torque (Fig. not presented) contributes to the generation of momentum over the Indian subcontinent, Western Indian Ocean off East Africa, North Africa and adjoining Arabian regions. The pressure torque dissipates momentum over the Arabian Sea, the Bay of Bengal, Central Indian Ocean and South China Sea. The forecasts capture these features reasonably well. Nevertheless, slight overestimation is noticed in the generation/dissipation of momentum during day 3 and day 5 forecasts.

The present work connotes that the omega momentum horizontal flux, the generation/dissipation due to pressure torque maintain the low level westerly flow against the loss of momentum to the atmosphere. The forecasts delineate the large scale balance of angular momentum fairly well though with reduced intensity due to systematic errors.

4. Conclusions

Based on the flow characteristics and comprehensive analysis of large scale dynamical balances, the following general conclusions can be drawn.

The model forecasts in all ranges (day 1 through day 5) delineate weakening of trans-equatorial flow into the Northern Hemisphere and southeasterly trades in the lower level (850 hPa) and weakening of Tibetan anti-cyclone and reduction of return flow into the Southern Hemisphere.

The forecasts represent the dynamical features associated with the summer monsoon realistically albeit with a reduced intensity. The study connotes that the monsoon domain is characterized as the source region of kinetic energy and vorticity. Both are produced in the monsoon region and transported horizontally across.

The forecasts underestimate the budget terms of mean and eddy kinetic energy. This is noticed from day 1 to day 5. However, this is pre-

dominant in the upper levels due to systematic weakening of return flow. It is interesting to notice the increasing tendency in the eddy to mean conversion of kinetic energy in the upper troposphere north of 40° N.

The forecasts represent the balance requirements in the vorticity budget fairly well, despite underestimation of the balance terms. Although, the net absolute vorticity advection weakens as the forecast process advances, the relative vorticity advection strengthens due to anomalous cyclonic circulation features in the flow characteristics..

The balance requirements in the angular momentum budget are represented reasonably well. However, the forecasts underestimate the budget terms. The angular momentum budget reveals that the flux transport of omega momentum into the monsoon region is imperative to maintain the surface westerlies against the friction. The analysis shows the flux divergence of omega momentum which confirms weaker surface westerlies over the monsoon region.

It is noticed that the model forecasts fail to maintain the analyzed atmospheric variability in terms of mean and transient eddy circulations over the monsoon region. Further, it is encapsulated from the study that the medium range forecasts enfeeble monsoon circulation due to deficiencies in the representation of significant physical processes such as convection and radiation. The representation of orography and parameterization of gravity wave drag in the model have to be improved in order to minimize the damping of transients.

Acknowledgements

The authors sincerely acknowledge the NCMRWF for providing the data and computing facilities to carry out this study. The authors are grateful to anonymous reviewers comments, which enabled to improve the manuscript significantly. This work is supported by office of Naval Research/Naval Research Laboratories, Washington D.C., U.S.A.

References

Alpert, J. C., Kanamitsu, M., Caplan, P. M., Sela, J. G., White, G. H., Kalney, E., 1988: Mountain induced wave drag parametrization in the NMC medium-range model, 8th Conference on Numerical Weather Prediction, Baltimore, Md., Feb. 22–26, 1988, American Meteorological Society, 252–259.

Chu, J. H., Yanai, M., Sui, C. H., 1981: Effects of cumulus convection on the vorticity field in the tropics. Part-I The large scale budget. *J. Meteor. Soc. Japan,* **59**(4), 535–546.

Fein, J. S., 1977: Global vorticity budget over the tropics and subtropics at 200 mb during the northern hemisphere summer. *PAGEOPH,* **115**, 1493–1500.

Haltiner, G. J., Williams, R. T., 1980: *Numerical Prediction and Dynamic Meteorology,* 2nd ed. New York: John Wiley & Sons.

Heckley, W. A., 1985a: Systematic errors of the ECMWF operational forecasting model in tropical regions. *Quart. J. Roy. Meteor. Soc.,* **111**, 709–738.

Heckley, W. A., 1985b: The performance and systematic errors of the ECMWF tropical forecasts (1982–1984). ECMWF Technical Report No: 53.

Holopainen, E. O., Oort, A. H., 1981: Mean surface stress curl over the oceans as determined from the vorticity budget of the atmosphere. *J. Atoms. Sci.,* **33**, 773–792.

Holopainen, E. O., Eerola, K., 1979: A diagnostic study of the long term balance of kinetic energy of atmospheric large scale motion over the British Isles. *Quart. J. Roy. Meteor. Soc.,* **105**, 849–858.

Holton, J. R., Colton, D. F., 1972: A diagnostic study of the vorticity balance at 200 mb in the tropics during the northern summer. *J. Atmos. Sci.,* **29**, 1124–1128.

Holton, J. R., 1992: *An Introduction to Dynamic Meteorology,* 3rd ed. Academic Press, (International Geophysics Series, vol. 48).

Kanamitsu, M., 1985: A study of the predictability of the ECMWF operational forecast model in the tropics. *J. Meteor. Soc. Japan,* **63**(5), 779–804.

Kanamitsu, M., 1989: Description of the NMC global data assimilation and forecast system. *Wea. Forecasting,* **4**, 335–342.

Krishnamurti, T. N., Ardanuy, P., Ramanathan, Y., Pasch, R., 1981: On the onset vortex of the summer monsoon. *Mon. Wea. Rev.,* **109**, 344–363.

Kung, E. C., 1966: Large scale balance of kinetic energy in the atmosphere. *Mon. Wea. Rev.,* **94**, 627–640.

Kung, E. C., 1971: A diagnosis of adiabatic production and destruction of kinetic energy by the meridional and zonal motions of the atmosphere. *Quart. J. Roy. Meteor. Soc.,* **97**, 61–74.

Kung, E. C., Smith, P. J., 1974: Problems of large scale kinetic energy balance, a diagnostic analysis in GARP. *Bull. Amer. Meteor. Soc.,* **55**, 768–777.

Kung, E. C., Beaker, W. E., 1975: Energy transformations in mid-latitude disturbances. *Quart. J. Roy. Meteor. Soc.,* **101**, 793–815.

Lorenz, E. N., 1967: The nature and theory of the general circulation of the atmosphere, First IMO lecture, WMO Tech Rep # 218, 161pp.

Mohanty, U. C., Dube, S. K., Singh, M. P., 1983: A study of heat and moisture budgets over the Arbian sea and their role in the onset and maintenance of summer monsoon. *J. Meteor. Soc. Japan,* **61**, 208–211.

Mohanty, U. C., Ramesh, K. J., 1994: A study on the dynamics and energetics of the Indian summer

monsoon. *Proceedings of the Indian National Science Academy,* **60**(A,1), 23–55.

Mohanty, U. C., Heckley, W. A., Ramesh, K. J., 1995a: A study on the systematic errors of the tropical forecasts. Influence of Physical processes. *Meteorol. Atmos. Phys.,* **55**, 151–166.

Mohanty, U. C., Das, S., Saseendran, S. A., et al. 1995b: Medium range prediction of Atmospheric system over Indian region by NCMRWF forecasting system. Proceedings of Fifth regional workshop on Asian/African monsoon emphasizing training aspects (WMO Tropical Meteorology Research Programme series Report No: 52, WMO/TD-NO: 698), 51–62.

O'Brien, J. J., 1970: Alternative solutions to classical vertical velocity problem. *J. Appl. Meteor.,* **9**, 197–203.

Parrish, D. F., Derber, J. C., 1992: The National Meteorological Centre's spectral statistical interpolation analysis system. *Mon. Wea. Rev.,* **120**, 1747–1763.

Pearce, R. P., 1979: On the concept of available potential energy. *Quart. J. Roy. Meteor. Soc.,* **104**, 737–755.

Pearce, R. P., Mohanty, U. C., 1984: Onsets of the Asian summer monsoon 1979–82. *J. Atmos. Sci.,* **41**(9), 1622–1639.

Rabier, F., Klinker, E., Courtier, P., Hollingsworth, A., 1996: Sensitivity of the forecast errors to initial conditions. *Quart. J. Roy. Meteor. Soc.,* **122**, 529, Part-A, 121–150.

Reed, R. J., Johnson, R. H., 1974: The vorticity budget of the synoptic-scale wave disturbances in the tropical western Pacific. *J. Atmos. Sci.,* **31**, 1784–1790.

Savijarvi, H., 1980: Energy budget calculations and diabatic effects for limited areas computed from ECMWF analyses and forecasts, Proceedings of the workshop: Diagnostics of diabatic processes, ECMWF, 115–134.

Savijarvi, H., 1981: The energy budgets in North America, North Atlantic and Europe based on ECMWF analyses and forecasts, ECMWF Tech Report No: 27.

Slingo, J. M., Mohanty, U. C., Tiedke, M., Pearce, R. P., 1988: Prediction of the 1979 summer monsoon onset with modified parameterization schemes. *Mon. Wea. Rev.,* **116**, 328–346.

Tiedke, M., Heckley, W. A., Slingo, J., 1988: Tropical forecasting at ECMWF: The influence of physical parametrization on the mean structure of forecasts and analyses. *Quart. J. Roy. Meteor. Soc.,* **114**, 639–664.

White, G. H., 1988a: On the performance of the NMC medium range forecast model in mid latitudes. Palmen Memorial Symposium on Extratropical Cyclones, Helsinki, Finland, 1988, American Met. Society, 305–308.

White, G. H., 1988b: The NMC model systematic errors in medium and extended range forecasts, Workshop on systematic errors in models in the atmosphere Toronto, Canada, 19–23 September 1988, 12, WMO/TD No. 273.

Author's addresses: P. L. S. Rao* and U. C. Mohanty, Centre for Atmospheric Sciences, Indian Institute of Technology, Hauz Khas, New Delhi-110016, India; K. J. Ramesh, National Centre for Medium Range Weather Forecasting (NCMRWF), Mausam Bhavan Complex, Lodi Road, New Delhi-110003, India. *Current Affiliation: IBM Solutions Research Centre, Indian Institute of Technology, Hauz Khas, New Delhi-110016, India.